ELSEVIER

Journal of Nuclear Materials 255 (1998) 222–233

journal of nuclear materials

Extension of the TRANSURANUS burnup model to heavy water reactor conditions

K. Lassmann *, C.T. Walker, J. van de Laar

European Commission, Joint Research Centre, Institute for Transuranium Elements, P.O. Box 2340, D-76125 Karlsruhe, Germany

Received 25 November 1997; accepted 23 January 1998

Abstract

The extension of the light water reactor burnup equations of the TRANSURANUS code to heavy water reactor conditions is described. Existing models for the fission of ^{235}U and the buildup of plutonium in a heavy water reactor are evaluated. In order to overcome the limitations of the frequently used RADAR model at high burnup, a new model is presented. After verification against data for the radial distributions of Xe, Cs, Nd and Pu from electron probe microanalysis, the model is used to analyse the formation of the high burnup structure in a heavy water reactor. The new model allows the analysis of light water reactor fuel rod designs at high burnup in the OECD Halden Heavy Water Reactor.

1. Introduction

The thermal and mechanical behaviour of a fuel rod depend strongly on complex phenomena that vary with burnup. Therefore, one of the first steps in describing fuel rod behaviour is to calculate at each fuel position the fraction of fissile material burnt (local burnup), the conversion of ^{238}U to ^{239}Pu and the subsequent buildup and fission of the higher Pu isotopes. The equations used constitute the so-called burnup models. Burnup is usually quoted as rod average burnup or as average burnup of a specific section (section average burnup) of the fuel rod. Both values are not to be confused with the local value.

In the present paper, the light water reactor (LWR) burnup equations of the TRANSURANUS code [1] are extended for heavy water reactor power stations (HWRs). Emphasis is placed on high burnup. This may seem to be contradictory since commercial HWRs use natural or only slightly enriched uranium and hence their burnup is limited to approximately 10 000 MWd/tU. However, the interest in HWRs in the context of high burnup stems from experimental HWRs such as the OECD-Halden Reactor [2] in which numerous instrumented LWR rods have been irradiated to high burnup and the results obtained used worldwide to validate fuel performance models. Two areas of special interest are as follows.

(a) The variation of the radial distributions of the fissile material with burnup which determines the radial power density distribution (and hence the radial burnup distribution) and the radial distribution of fission products such as Kr, Xe, Cs and Nd.

(b) The formation of the high burnup structure (HBS).

The formation of the high burnup structure in a HWR has never been studied and is the central aspect of this paper. Generally, the formation of the high burnup structure is characterised by:

(a) a decrease in the UO_2 grain size (the development of a subgrain microstructure),

(b) the development of fission gas pores (formation of a new pore structure in the HBS),

(c) xenon depletion of the matrix (athermal release of Xe from the original UO_2 grains).

Although the physical details are not fully understood, an attempt has been made to describe these processes by a simple physical model [3]. The key parameter is the local burnup which is mainly determined by the fission of ^{235}U, ^{239}Pu and ^{241}Pu. The process of fission is nonuniform along the pellet radius since a higher concentration of plutonium ^{239}Pu is formed by resonance absorptions in

* Corresponding author.

0022-3115/98/$19.00
PII: S0022-3115(98)00019-1

^{238}U near the surface of the pellet. The result is that with increasing irradiation time, the local burnup near the surface becomes much higher than the average burnup of the fuel.

Two local threshold burnups can be identified:

(a) a local threshold burnup for the transition of the original grain structure to the formation of local HBS spots (approximately 60,000 MWd/tU),

(b) a local threshold for the fully developed HBS (approximately 75,000 MWd/tU).

For typical LWR conditions, these local thresholds correspond to a section average burnup of approximately 40 000–45 000 MWd/tU. At this average burnup, the formation of the HBS starts at the surface of the fuel pellet. This is sometimes mistakenly referred to as the 'rim effect' in LWR fuel, see, e.g., Ref. [4]. For the Halden Reactor, it is claimed that the formation of the HBS starts at a higher section average burnup because less neutrons are captured in the resonances of ^{238}U and hence less fissile Pu is created. Thus, the HBS should form later in the life of a fuel rod irradiated in the Halden Reactor or any other HWR and it seems worthwhile to attempt to quantify this effect.

In this paper, the existing models for the fission of ^{235}U and the buildup of plutonium in a HWR are evaluated. In order to overcome the limitations of the frequently used RADAR model at high burnup, a new model is presented. After verification against data for the radial distribution of Xe, Cs, Nd and Pu from electron probe microanalysis (EPMA) the formation of the HBS in a heavy water reactor is analysed.

2. Current theoretical models for the buildup of plutonium

Models currently available to describe the local buildup of plutonium in a fuel pin irradiated in a HWR are those of Carlsen and Sah [5], the RADAR model ('RAting Depression Analysis Routine') of Palmer et al. [6] and an extension of the TRANSURANUS burnup model [7] for HWR conditions developed by Lemehov [8]. Unfortunately, it is not possible to use the latter model because some details cannot be understood and verified.

The model of Carlsen and Sah consists of one equation for ^{239}Pu, whereas the RADAR model is based on two differential equations; one for the ^{235}U concentration, the other for the ^{239}Pu concentration. Both models use simple diffusion theory to obtain the radial distribution of the thermal flux and, in both models, the generated plutonium is distributed radially according to an empirical function which keeps the model simple.

The widely used RADAR model offers distinct advantages over that of Carlsen and Sah; it is very flexible and can be used for LWR and HWR conditions since characteristic reactor quantities such as the fast leakage factor and the resonance escape probability are input data. The main disadvantage of both models is that they take only the formation of ^{239}Pu into account, i.e., the formation of ^{240}Pu and higher Pu isotopes is neglected.

Two versions of the RADAR model have been analysed; the original version (RADAR) and a specific version for use in Halden irradiations (RADAR-HWR) recommended by Wiesenack [9] who advocates the use of a specific correlation for the inverse diffusion length, κ, used in the radial flux distribution:

$$\Phi(r) \propto I_0(\kappa r), \tag{1}$$

where Φ is the thermal neutron flux and I_0 is the modified Bessel function of order zero. The correlation recommended by Wiesenack for κ is:

$$\kappa = 32.8(E\rho)^{0.8} + 54\left(\frac{5}{R}\right)^{0.82} \times (E\rho)^{0.19} \quad \left[\frac{1}{m}\right]. \tag{2}$$

This correlation, also given in Ref. [5], has been widely used in the Halden project. E is the ^{235}U enrichment (%), R the fuel radius (mm) and ρ the fractional density of the fuel.

For both versions, the same specific details of the Halden reactor were used; a resonance escape probability of 0.92 and a fast leakage factor of 0.975.

3. The new TRANSURANUS-HWR burnup model

The new TRANSURANUS-HWR burnup model is an extension of the LWR burnup model of the TRANSURANUS code [1]. The burnup equations of the TRANSURANUS-LWR burnup model [7] are based on the concept of one group, spectrum-averaged cross-sections which is also used in codes like ORIGEN [10] and KORIGEN [11]. As in all other models, the radial distribution of plutonium is obtained from an empirical shape function. The basic equations are

$$\begin{aligned}
\frac{\mathrm{d}N_{235}(r)}{\mathrm{dbu}} &= -\sigma_{\mathrm{a},235}\, N_{235}(r)\, A,\\
\frac{\mathrm{d}N_{238}(r)}{\mathrm{dbu}} &= -\sigma_{\mathrm{a},238}\, \bar{N}_{238}\, f(r)\, A,\\
\frac{\mathrm{d}N_{239}(r)}{\mathrm{dbu}} &= -\sigma_{\mathrm{a},239}\, N_{239}(r)\, A + \sigma_{\mathrm{c},238}\, \bar{N}_{238}\, f(r)\, A,\\
\frac{\mathrm{d}N_{j}(r)}{\mathrm{dbu}} &= -\sigma_{\mathrm{a},j}\, N_{j}(r)\, A + \sigma_{\mathrm{c},j-1} N_{j-1}(r)\, A,
\end{aligned} \tag{3}$$

where $\sigma_{\mathrm{a},i}$ and $\sigma_{\mathrm{c},i}$ are the neutron absorption and capture

cross-sections, respectively, and the index j stands for the isotopes 240, 241 and 242. 'A' is a conversion constant (for details, see Ref. [6], Eq. 3) and $Nj(r)$ is the local concentration of the isotope j. The local concentration of ^{238}U is written as $\bar{N}_{238}\ f(r)$ where $f(r)$ is a normalised radial shape function which encapsulates the contribution of the resonance absorption to the total plutonium production. It is a function of the form

$$f(r) = 1 + p_1 e^{-p_2(R-r)^{p_3}}, \tag{4}$$

where R is the fuel radius and p_1, p_2 and p_3 are constants. The values of these constants were derived after careful and exhaustive comparisons with measurements. The input model parameters are the fuel geometry (inner and outer radius), porosity, ^{235}U enrichment and initial concentrations of the plutonium isotopes.

The equations outlined above are solved incrementally. For each average burnup increment, a new radial power density profile is calculated from which the radial burnup profile is updated. Finally, the local concentrations of Kr, Xe, Cs and Nd are obtained by multiplying the local burnup increment by the appropriate fission yields.

The TRANSURANUS-LWR burnup model has been verified against a large LWR database of spent fuel measurements for enrichments in the range 1.38–8.25% and for burnups between 20 000 and 85 000 MWd/tU. It has been independently assessed by Battelle Northwest and has been incorporated into the new version of the FRAPCON-3 code [12].

The first step in the development of a HWR version is the determination of the one group, spectrum-averaged cross-sections for neutron absorption and capture used in Eq. (3). For the development of the present simple model, these were estimated from the neutron spectrum of the Halden HWR [13] which differs significantly from that of a LWR: in the Halden Reactor, the thermal flux is higher and the fast flux is lower than in a typical LWR (see Fig. 1).

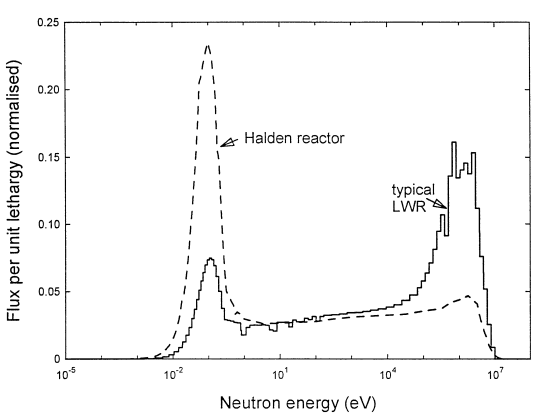

Fig. 1. Comparison between the neutron spectra of the Halden HWR [13] and a commercial LWR.

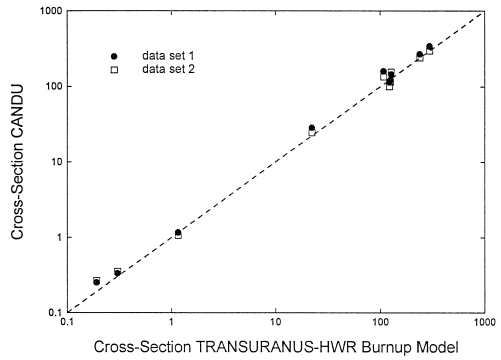

Fig. 2. Comparison between the one group, spectrum-averaged cross-sections of the new TRANSURANUS-HWR burnup model and two data sets for the CANDU HWR given in the OECD/NEA JEF-2.2 data libraries [14].

The one group, spectrum-averaged cross-sections can be defined as

$$\sigma = \frac{\int_0^\infty \sigma'(E)\Phi(E)\mathrm{d}E)}{\int_0^\infty \Phi(E)\mathrm{d}E}. \tag{5}$$

For σ'(E), the OECD/NEA, JEF-2.2 standard libraries were used [14]. Care was taken to make sure that the resonances in the epithermal region were taken into account.

The results can be compared with one group cross-sections for a CANDU (HWR) from the same reference. As can be seen from Fig. 2, the results of the very simple approach adopted here agree well with the cross-sections in the OECD/NEA library which are based on detailed neutron physics methods.

The simple approach can also be used to estimate the relative contribution of the epithermal region to the total effective cross-section. For a LWR this number is approximately 0.44, whereas for a HWR a lower value of approximately 0.28 is obtained. This means that in a HWR less neutrons are captured in the epithermal region than in a LWR.

This quantitative information is used to modify the radial shape function, $f(r)$, calculated with Eq. (4). The second term in this equation describes the relative contribution of neutron capture in the epithermal region and accordingly

$$p_1^{\mathrm{HWR}} = 0.64\, p_1^{\mathrm{LWR}}. \tag{6}$$

It will be shown later that Eq. (6) is in agreement with the data.

The modification of the cross-sections and the modification of the constant p_1 are the only differences compared with the LWR version and constitute the new TRANSURANUS-HWR burnup model. The model is con-

tained in the subroutine TUBRNP which can be run as a stand-alone program or as part of the TRANSURANUS code. When run as a stand-alone program, processes such as thermal fission gas release are not modelled.

4. Comparison of the RADAR model and the TRANSURANUS model

From what has been said above, it can be deduced that good agreement between the HWR versions of the RADAR model and the TRANSURANUS-HWR burnup model is to be expected when the fission of uranium dominates (i.e., at low burnup, or at high burnup when the initial U enrichment is high) whereas differences are to be expected if the fission of plutonium dominates (e.g., at high burnup when the initial U enrichment is low and when the buildup of the higher Pu isotopes is relevant and has to be taken into account).

A detailed comparison was made for various pin designs (PWR and BWR) at a section average burnup of 50 000 MWd/tU and this confirmed the general expectations. No significant difference between PWR and BWR pins was found. Also, the difference between the two different versions of the RADAR model (RADAR—Halden version and the original version) is very small. Clearly, these details are not relevant at high burnup where the major effect comes from the buildup of plutonium near the fuel surface. In order to show the main differences between the RADAR model and the TRANSURANUS-HWR burnup model, a few examples from the comparison are given. Fig. 3 shows the predicted radial distribution of plutonium. As can be seen, at the relatively low enrichment of 3% the difference in the predicted plutonium buildup is large. A comparison of the predicted burnup profiles was made by comparing the calculated radial neodymium profiles (Fig. 4). The agreement between both models is reasonable since similar concentrations were obtained for the fissile isotopes (basically, ^{235}U and ^{239}Pu). However, one characteristic behaviour of the new TRANSURANUS-HWR burnup model can already be

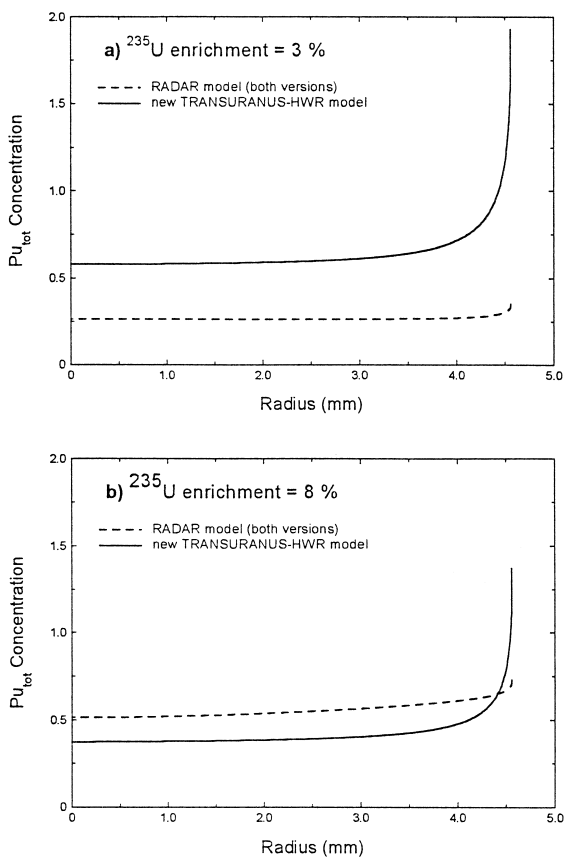

Fig. 3. Radial distribution of plutonium as predicted by the RADAR model and the new TRANSURANUS-HWR burnup model: (a) 3% ^{235}U enrichment; (b) 8% ^{235}U enrichment. Section average burnup 50 000 MWd/tU.

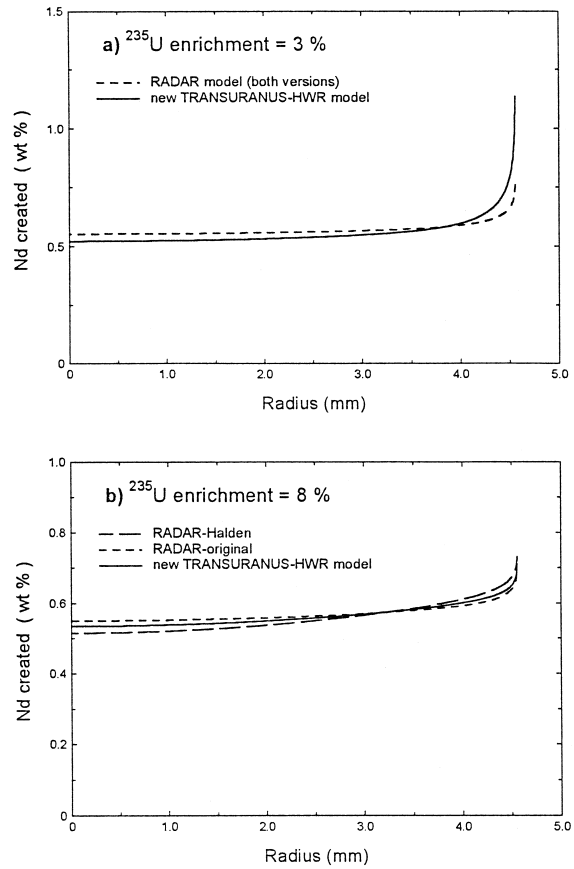

Fig. 4. Radial distribution of neodymium as predicted by the RADAR model and the new TRANSURANUS-HWR burnup model: (a) 3% ^{235}U enrichment; (b) 8% ^{235}U enrichment. Section average burnup 50 000 MWd/tU.

seen: when the fission of converted plutonium dominates, it predicts higher concentrations near the fuel surface than the RADAR model. This feature is given particular attention in the verification of the model reported in Section 5.

5. Validation of the new TRANSURANUS-HWR burnup model

5.1. Data used

The HWR fuel sections employed in the validation of the new TRANSURANUS-HWR burnup model are listed Table 1. With the exception of those for sections AG17-4 and M2-2C, all the results for the radial distribution of Xe, Cs, Nd and Pu were obtained by electron probe microanalysis at the Institute for Transuranium elements carried out by one of the authors (CTW).

5.1.1. Radial profiles from fuels irradiated in the Danish research reactor DR3

Five specimens were irradiated in the Danish research reactor DR3:

Specimens AG17-4 ($\approx$ 20,000 MWd/tU) and M2-2C ($\approx$ 41 000 MWd/tU) are documented in Ref. [5]. On both sections, α-autoradiography was used to estimate the relative radial concentration of alpha emitters, which is considered to reflect the distribution (but not the absolute value) of ^{239}Pu and ^{241}Pu. Therefore, these results can be used in the normalised form only.

Section AF21-2-8 was irradiated to more than 70,000 MWd/tU. The irradiation took place in a special light water rig, which leads to a neutron spectrum somewhere between light and heavy water conditions [15]. This is also an interesting irradiation because the initial enrichment was very low (1.5%), i.e., most of the fission is based on converted plutonium. The difference between a LWR and a HWR spectrum should therefore diminish since most of the fissile material is created by the same physical process.

Four radial EPMA profiles are available from the D-COM coordinated research programme for development of computer models for fuel element behaviour in water reactors sponsored by the IAEA [16,17]. In this program three miniature rods, AG11-8, AG11-9 and AG11-10, were irradiated together as test HP 096. The rods AG11-9 and AG11-10 were subsequently transient tested together as test HP 129. Caesium and xenon profiles are available from rods AG11-8 and AG11-10.

5.1.2. Radial profiles from fuels irradiated in the OECD Halden Reactor

Several radial electron probe microanalysis profiles are available from the first Risø Fission Gas Project [18]. In this project, 12 fuel pins were irradiated in the Halden

Table 1
The HWR fuel sections employed in the verification of the new TRANSURANUS-HWR burnup model; note that the burnup has been converted from rounded values given in at.%

	Section	Radius (mm)	Enrichment (%)	Burnup (MWd/tU)	Radial profile available
Risø irradiation DR3	AG17-4-II	4.645	3.16	19 792	Pu
	M2-2C-I	6.3	2.28	41 204	Pu
	AF21-2-8	6.14	1.5	72 239	Nd, Pu, Xe
DCOM [16] DR3	AG11-10-8	4.645	2.28	32 000	Cs, Xe
	AG11-8-11	4.645	2.28	32 000	Cs, Xe
Risø 1 [18] Halden: IFA-148	F14-6-44	6.3	5.0	32 720	Xe
	F14-6-56	6.3	5.0	37 265	Xe
	F9-3-44	6.3	5.0	39 083	Nd, Xe
	F9-3-48	6.3	5.0	38 174	Xe
	F9-3-82	6.3	5.0	35 447	Xe
	G3-2-10	6.3	5.0	33 629	Xe
	G3-2-15	6.3	5.0	36 356	Xe
	G3-2-19	6.3	5.0	34 538	Xe
	M1-3-11	6.3	5.0	39 992	Xe
Risø 2 [19] Halden: IFA-161	M23-1-17R-3	6.3	5.078	31 811	Cs, Pu, Xe
	M23-1-21R-3	6.3	5.078	49 989	Cs, Pu, Xe
	M23-1-6-6	6.3	5.078	41 809	Cs, Pu, Xe
	M23-1-9-6	6.3	5.078	43 627	Cs, Pu, Xe
	M72-2-2R-12	6.3	5.078	43 627	Cs, Xe
	M72-2-7R-15	6.3	5.078	47 263	Cs, Xe
	M78-1-12	6.3	5.078	31 811	Cs, Xe
	M78-1-19	6.3	5.078	48 171	Cs, Xe
	M78-1-32	6.3	5.078	37 265	Cs, Xe (2 each)

Table 2
EPMA Conditions used for the quantitative analysis of Xe, Cs, Nd and Pu

Element	X-ray line	Diffracting crystal	Eo (kV)	Beam current (nA)	Counting time, s		Standard
					Peak	Background	
Xe	$L\alpha_1$	Quartz 1011	25	250	50	50	Sb
Cs	$L\beta_1$	LiF	25	250	50	50	CsI
Nd	$L\alpha_1$	LiF	25	250	50	50	Nd
Pu	$M\beta$	Quartz 1011	25	100	25	25	PuO_2

Reactor, a boiling heavy-water reactor, to an assembly average burnup of 32 000 MWd/tU. The irradiation was designated IFA-148 and started in February 1968. Shutdown was in August 1979, i.e., the pins were 11.5 years in the reactor. After this base-irradiation some of the rods were submitted to short-term re-irradiations at increased power levels, so-called bump tests, in the DR3 reactor. The average burnup in these sections ranges from approximately 32 000 to 40 000 MWd/tU.

The remaining radial profiles originate from the second Risø project, the 'Risø Transient Fission Gas Release Project' [19]. Risø and General Electric supplied the test fuel for this project. The Risø fuel that is of interest here was base-irradiated in the Halden Reactor as irradiation IFA 161 to an average burnup between 30 000 and 48 000 MWd/tU. The irradiation started in July 1968 and ended in October 1981, i.e., the irradiation lasted for more than 13 years. After this base-irradiation, several short rods were refabricated, instrumented with pressure transducers and were transient tested in the DR3 reactor.

In total, 12 radial caesium profiles, 2 neodymium profiles, 7 plutonium profiles and 22 xenon profiles were

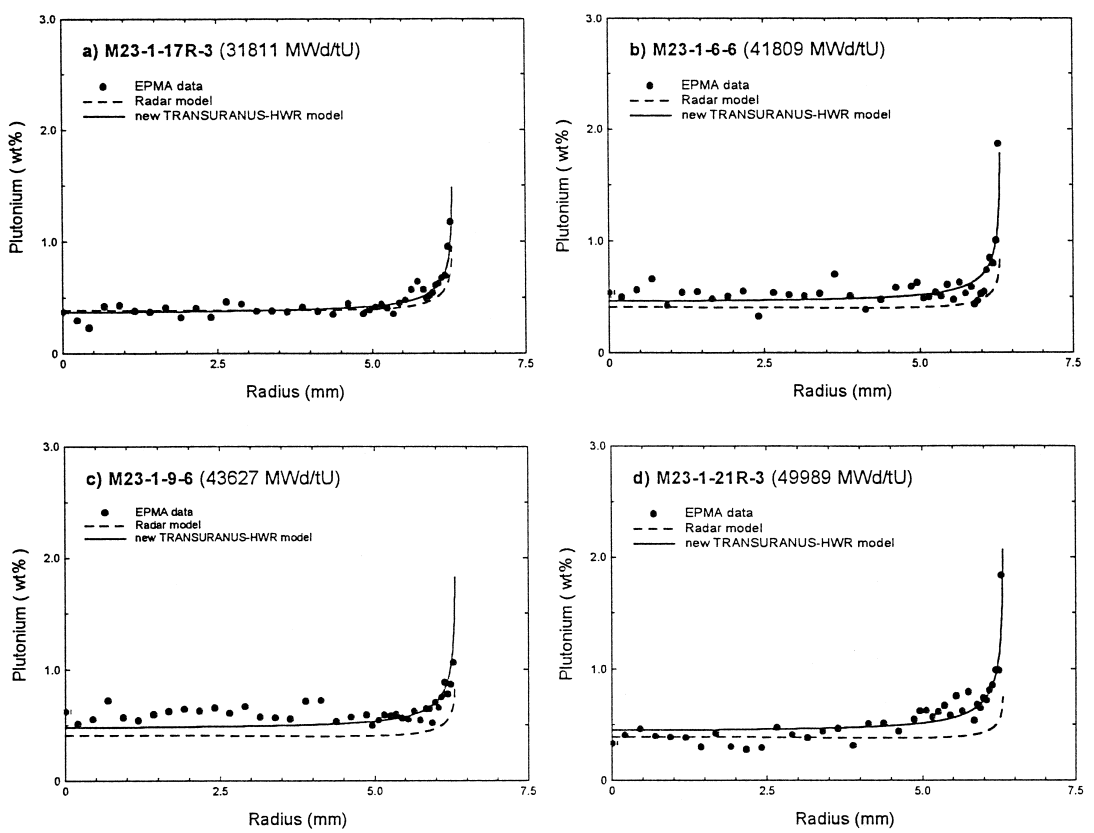

Fig. 5. Comparison of the measured radial plutonium profile with that calculated by the RADAR model and the new TRANSURANUS-HWR burnup model.

available for the verification of the new TRANSURANUS-HWR burnup model.

5.2. Electron probe microanalysis

Electron probe microanalysis was carried out on a Cameca MS46 electron microprobe shielded with tungsten and lead to permit the analysis of irradiated nuclear fuel [20]. The analysis conditions used for Xe, Cs, Nd and Pu are summarised in Table 2. It is seen that a high electron acceleration potential and high beam current was used for the analysis of Xe, Cs and Nd. This ensured good counting statistics, a low detection limit and that the depth of electron penetration was sufficient to avoid surface effects. To decrease the radiation background, the pulse height analyser was used in the differential mode. The EPMA matrix correction was made using the QUAD2 program of Farthing et al. [21], which is based on the Quadrilateral Model of Scott and Love [22]. For U, *k*-ratios measured at the same locations as the elements of interest were input; for oxygen a fixed concentration of 11.8 wt% was used.

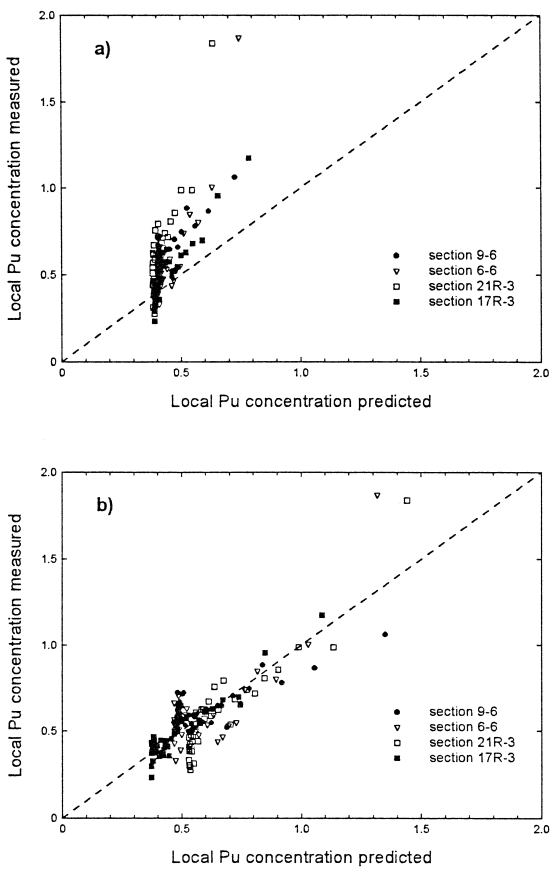

Fig. 6. Comparison of the local Pu measured by EPMA with the concentrations predicted by (a) the RADAR model, and (b) the new TRANSURANS-HWR burnup model for different fuel sections from rod M231 (^{235}U enrichment 5.1%).

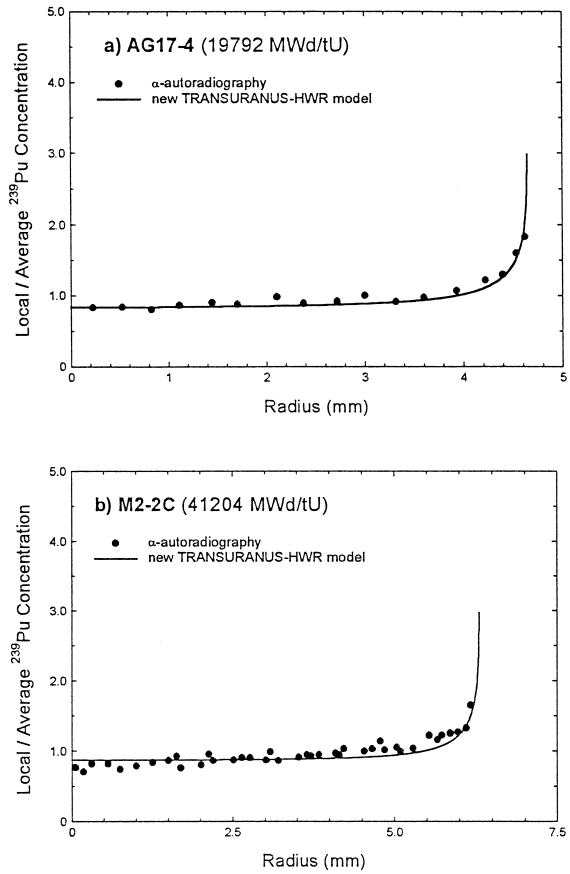

Fig. 7. Comparison of the measured radial plutonium profile in normalised form with that calculated by the new TRANSURANUS-HWR burnup model.

The analysis procedures used for Xe, Cs and Pu are described in detail in Refs. [23–25,7]. For the analysis of Xe an Sb standard was used and a correction factor applied. A crystal of CsI was used as a standard for Cs. Caesium iodide is unstable under the electron beam, and hence the determinations on the standard were made at a reduced beam current of 50 nA and the counting time was restricted to 10 s. Since the U Mβ line interferes with the Pu $M\alpha_1$ line, the Pu Mβ line was used for the analysis of Pu. This line, however, is not interference free; the relatively minor U $M\gamma_2$ line interferes with the Pu Mβ line. The intensity of the Pu Mβ line was corrected for X-ray contributions from the overlapping U $M\gamma_2$ line as described in Ref. [7].

Around 40 points were used to construct the radial distribution profiles of Xe, Cs, Nd and Pu. The first point was located nominally 10 μm from the pellet rim, the rest

were spaced at intervals of 50 to 250 μm along the pellet radius. At each location, the concentration of Pu was determined from the average of four peak and three background measurements, and the concentrations of Xe, Cs and Nd from the average of six peak and four background determinations. The specimen current image (absorbed electron current) was used to obtain information about the fuel microstructure at the locations selected for analysis and to position the electron beam.

The confidence interval on the measured Xe concentrations at a significance level of 99% is about 5% relative at a concentration of 0.5 wt% and 10–20% relative at 0.05 wt%. For Nd and Cs, similar levels of uncertainty are expected. In the case of Pu, the confidence interval on a measured concentration of 2.0 wt% is about 20% relative at a significance level of 99%. This large uncertainty is due to the application of a correction for use of a compound standard and the need to correct for X-ray contributions from the U $M\gamma_2$ line.

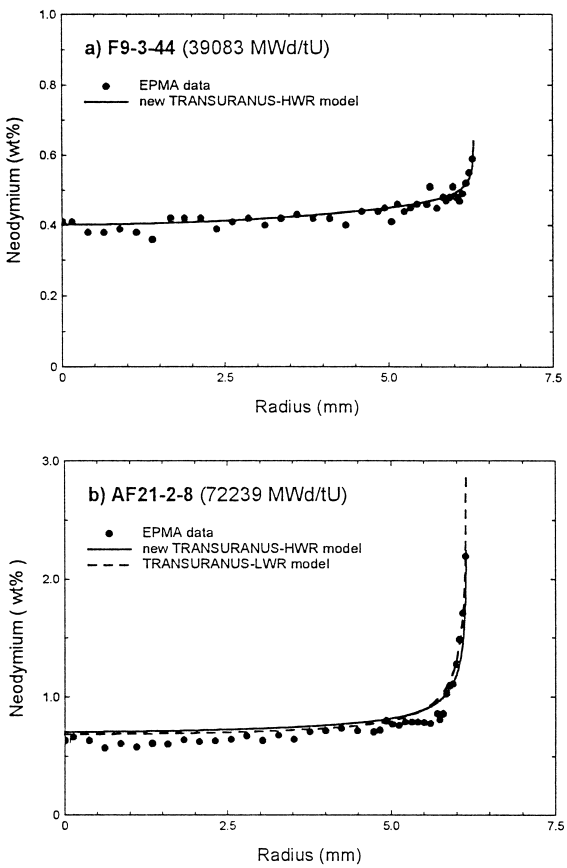

Fig. 8. Comparison of the measured radial neodymium profile with that calculated by the new TRANSURANUS-HWR burnup model. The radial neodymium profile calculated with the TRANSURANUS-LWR model is included in the plot (b) for the purposes of comparison.

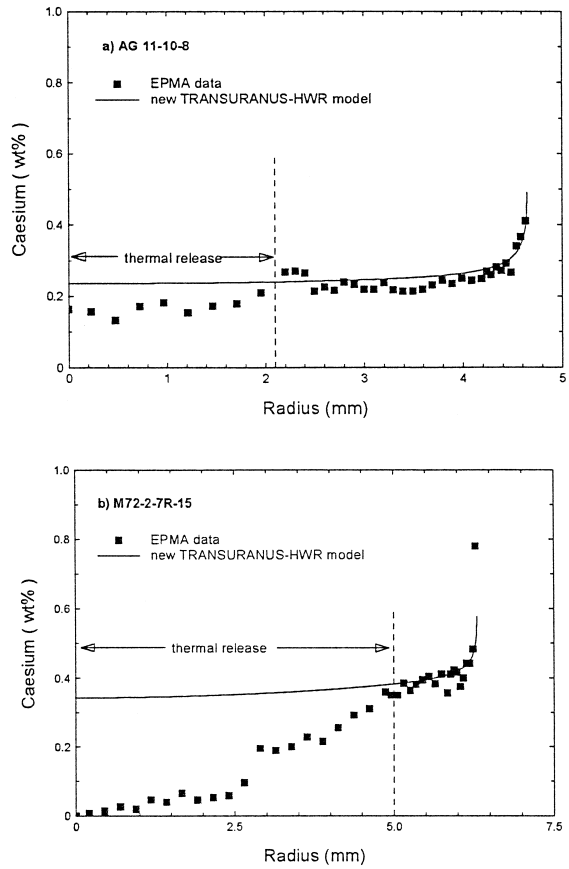

Fig. 9. Comparison between predicted and measured radial caesium concentration for two different cross-section average burnups: (a) 32 000 MWd/tU and (b) 47 263 MWd/tU.

5.3. Comparison between experimental and theoretical results

Both, the RADAR model and the new TRANSURANUS-HWR burnup model give the local concentration of plutonium. The RADAR model, however, calculates only ^{239}Pu, whereas the TRANSURANUS model gives the total plutonium as the sum of ^{239}Pu, ^{240}Pu, ^{241}Pu and ^{242}Pu. In Fig. 5a–d, the experimental results for the radial Pu distribution are compared with the predictions of both models for rod M23-1. It is to be noted that no normalisation has been carried out. Clearly, the TRANSURANUS-HWR burnup model gives better agreement than the RADAR model, which underpredicts the plutonium concentration near the surface. To emphasis this fact, the measured local Pu concentration has been plotted against the predicted concentrations in Fig. 6.

As explained in Section 5.1.1, the experimental results of Carlsen and Sah [5] obtained by α-autoradiography can only be used in the normalised form. One drawback of the technique is the large diametral spot size, which is esti-

mated to be of the order of 15 μm (A. Lagerwaard, personal communication). This means that with α-autoradiography the steep gradient at the pellet rim cannot be fully measured. That is to say, this technique is not able to reveal the details of the plutonium distribution near the fuel surface. However, it is seen from Fig. 7 that the predictions of the new TRANSURANUS-HWR burnup model are in general agreement with these measurements.

Neodymium profiles provide an excellent representation of the radial burnup distribution. One profile at a section average burnup of 39 083 MWd/tU (F9-3-44) and one at 72 239 MWd/tU (AF21-2-8) are available. As can be seen from Fig. 8, the agreement between the predictions of the new TRANSURANUS-HWR burnup model and the EPMA data are excellent. It is pointed out that again normalisation has not been used. As mentioned in Section 5.1.1, fuel section AF21-2-8 was irradiated in a neutron spectrum that was somewhere between light and heavy water conditions. Because of the low initial enrichment no major differences between the two conditions are expected. Fig. 8b confirms this and it is seen that the predictions made with both versions of the TRANSUANUS burn-up model are in good agreement with the EPMA data.

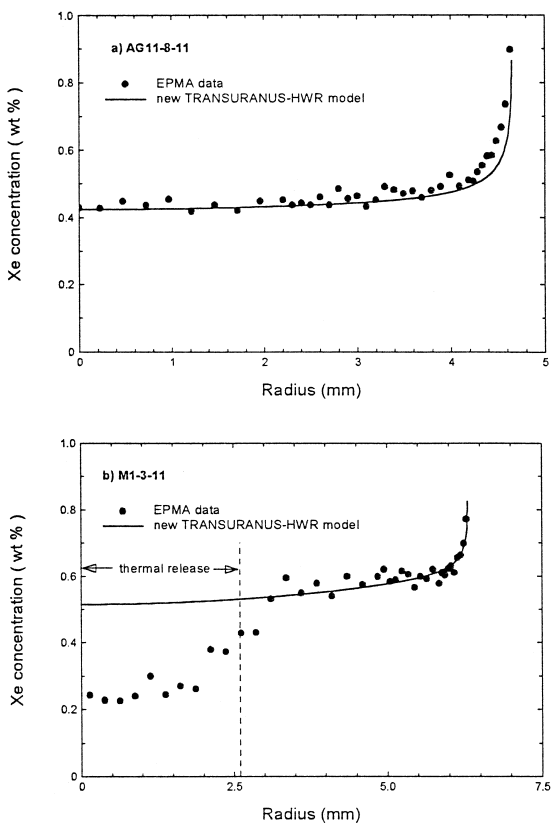

Fig. 10. Comparison between predicted and measured radial xenon concentration for two different cross-section average burnups: (a) 32 000 MWd/tU and (b) 39 992 MWd/tU.

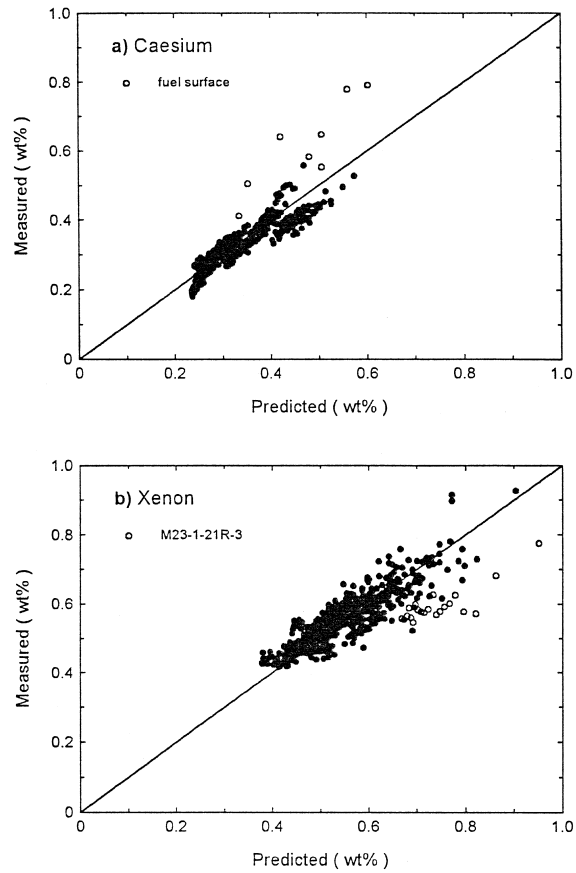

Fig. 11. Comparison between all predicted and measured Cs and Xe data omitting AF21-2-8. Only data points not affected by thermal fission gas release are considered.

Insufficient space is available to compare all the 12 measured Cs profiles and the 22 measured Xe profiles with the predictions of the new TRANSURANUS-HWR burnup model. Instead four typical examples are shown in Figs. 9 and 10. Since the stand-alone version of the new TRANSURANUS-HWR burnup model was used, thermal fission gas release is not accounted for. It is seen that the new model predicts reasonably well the created concentrations of Xe and Cs in the region not affected by thermal fission gas release.

In Fig. 11, all the predicted and measured local concentrations of Cs and Xe are compared at positions where thermal fission gas release did not occur. Xe data from section AF21-2-8 which exhibits the HBS have not been included. They will be discussed in detail in the next chapter. Those sections that had been transient-tested show a slight underprediction of the Cs concentration at the fuel surface. It is assumed that Cs released from the inner parts of the fuel has condensed on the surface. In contrast, Xe appears to be overpredicted at high burnup. However, this is mainly attributable to the data from a single section,

M23-1-21R-3. The reason for this deviation is unknown. It could be explained by frequent reactor shut-downs during the irradiation resulting in a higher decay of ^{133}Xe and ^{135}Xe to ^{133}Cs and ^{135}Cs and less transmutation to ^{134}Xe and ^{136}Xe due to neutron capture. Fig. 11 confirms that the new TRANSURANUS-HWR burnup model is consistent with the experimental evidence. The spread in the local concentrations measured by EPMA has been observed before (see, e.g., Ref. [3]) and is mainly attributed to uncertainties in the EPMA measurements, uncertainties in the burnup determination and also in the radial position of the data points close to the fuel surface. At a section average burnup of 50 000 MWd/tU, the concentration gradient near the surface is so steep that a variation of a few μm in the radial position may vary the local burnup by up to 20 000 MWd/tU.

6. Analysis of the high burnup structure of fuel irradiated in a HWR

Section 5 has shown that the new TRANSURANUS-HWR burnup model can predict reasonably well the radial Pu and burnup profiles and hence the Xe, Cs, Nd and Pu profiles. In order to get an indication of whether the HBS also exists in fuel irradiated in HWRs, the local Xe concentration in the UO_2 matrix as measured by EPMA is plotted as a function of the local burnup as calculated by the new model Fig. 12). Only Xe concentrations not affected by thermal fission gas release are considered. The result is very similar to that for LWR conditions (e.g., Ref. [1], Fig. 4). A more or less linear behaviour up to the threshold burnup is followed by a sharp decrease of Xe in the matrix, which denotes the formation of the HBS.

A simple model that describes the xenon depletion of the matrix (athermal release of Xe from the UO_2 grains) has been derived in Ref. [3]. The assumption is made that the loss term of Xe from the matrix to the newly developing pores is proportional to the Xe concentration:

$$\frac{\mathrm{dXe}}{\mathrm{dbu}} = -a\mathrm{Xe} + \dot{c}_{\mathrm{Xe}}, \tag{7}$$

where $\dot{c}_{\mathrm{Xe}}$ is the Xe creation rate and a is a fitting constant which is derived from the Xe equilibrium for $\mathrm{bu} \to \infty$ given by

$$\mathrm{Xe}_{\infty} = \frac{\dot{c}_{\mathrm{Xe}}}{a}. \tag{7a}$$

The solution of this differential equation is not straightforward since the total fission yield of Xe is not constant. It depends on whether:

(a) uranium or plutonium is fissioned,

(b) the unstable Xe isotopes 133 and 135 decay to the stable Cs isotopes 133 and 135 or are transmuted to the stable Xe isotopes 134 and 136. This in turn depends on the neutron flux and the number of reactor shut downs.

These details are taken into account in the TRANSURANUS burnup model, i.e., Eq. (7) is solved numerically.

However, in order to obtain some physical understanding, it is assumed that for all data, the Xe fission yield may be *approximated* by 0.268. With this assumption, Eq. (7) can be integrated:

$$\begin{aligned} \mathrm{Xe}(\mathrm{bu}) &= \dot{c}_{\mathrm{Xe}}\mathrm{bu} && \mathrm{bu} < \mathrm{bu}_0, \\ \mathrm{Xe}(\mathrm{bu}) &= \dot{c}_{\mathrm{Xe}}\left[\frac{1}{a} + \left(\mathrm{bu}_0 - \frac{1}{a}\right)e^{-a(\mathrm{bu}-\mathrm{bu}_0)}\right] && \mathrm{bu} \geq \mathrm{bu}_0, \end{aligned} \tag{8}$$

where bu_0 is the threshold burnup. This approximation is included in Fig. 12. It is stressed again that the

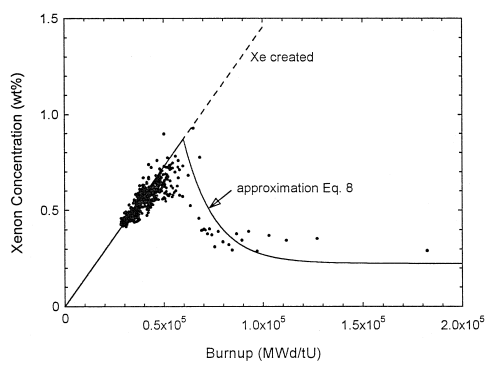

Fig. 12. Comparison between predicted and measured local xenon concentrations in the UO_2 matrix as a function of the local burnup. Only data points (536 in total) not affected by thermal fission gas release are considered. The threshold burnup is set at 60 000 MWd/tU.

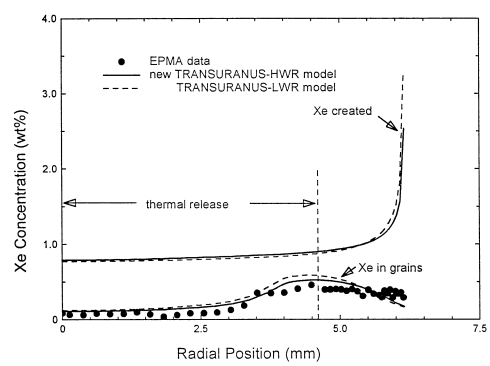

Fig. 13. Comparison between predicted and measured radial xenon concentration for fuel section AF21-2-8 (72 239 MWd/tU). The threshold burnup is set at 60 000 MWd/tU.

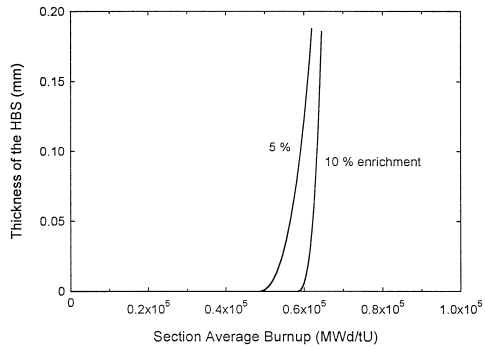

Fig. 14. Prediction of the thickness of the HBS (rim zone) in a HWR as a function of the section average burnup for ^{235}U enrichments of 5 and 10%. The results refers to a 'typical' PWR rod design and do not represent specific rod designs used to quickly achieve high burnup.

TRANSURANUS burnup model takes the details of fission yield into account.

Of particular interest is the high burnup section AF21-2-8. Since irradiation data have been made available by Kinoshita (personal communication), this irradiation could be analysed with the TRANSURANUS code into which the new HWR burnup model together with the model for the Xe depletion, Eq. (7), has been integrated. As in the case of Nd, the Xe profile of section AF21-2-8 has been analysed with the HWR and the LWR burnup models (Fig. 13). Differences between the predictions obtained with the two versions are small. There is only a slight overprediction of the gas measured in the grains and the general trend is reproduced reasonably well. It is interesting to note that at a radius around 4.5 mm two simultaneous processes must be considered: thermal fission gas release and Xe depletion due to the formation of the HBS. The former is calculated by the TRANSURANUS standard fission gas release model. The modelling of both these simultaneous and overlapping processes seems to be correct. However, this still needs further attention.

It is clearly evident from the results in Figs. 12 and 13, that the new TRANSURANUS-HWR burnup model can be used with confidence to estimate the thickness of the HBS as a function of the section average burnup in a fuel rod irradiated in a HWR. In the present model, the formation of the HBS depends on the initial composition of fissile material, fuel geometry, section average burnup and the burnup threshold. Fig. 14 gives two typical results for a PWR design with U enrichments of 5 and 10%. As can be seen, the formation of the HBS starts at a section average burnup of approximately 50 000 MWd/tU (5% U enrichment) and 60 000 MWd/tU (10% U enrichment) which is at least 10 000 MWd/tU higher than in a LWR irradiation.

Thus, the high burnup UO_2 structure should also be seen in fuel irradiated in a heavy water reactor, for instance in the OECD-Halden Reactor.

Acknowledgements

George Nicolaou gave helpful information on the KORIGEN and ORIGEN codes, Joe Magill provided the cross-section libraries and Jose Spino and Claudio Ronchi read the paper and gave valuable comments for its improvement. The contributions of all colleagues are gratefully acknowledged.

References

[1] K. Lassmann, J. Nucl. Mater. 188 (1992) 295.
[2] W. Wiesenack, Nucl. Eng. Design 172 (1997) 83.
[3] K. Lassmann, C.T. Walker, J. van de Laar, F. Lindström, J. Nucl. Mater. 226 (1995) 1.
[4] J.P. Piron, B. Bordin, G. Geoffroy, C. Maunier, D. Baron, Proceedings of the 1994 International Topical Meeting on Light Water Reactor Fuel Performance, West Palm Beach, FL, 1994, p. 321.
[5] H. Carlsen, D.N. Sah, Nucl. Technol. 55 (1981) 587.
[6] I.D. Palmer, K.W. Hesketh, P.A. Jackson, Water Reactor Fuel Element Performance Computer Modelling, Applied Science Publ., 1983, p. 321.
[7] K. Lassmann, C. O'Carroll, J. van de Laar, C.T. Walker, J. Nucl. Mater. 208 (1994) 223.
[8] S.E. Lemehov, Proceedings 1997 International Topical Meeting on Light Water Reactor Fuel Performance, Portland, OR, 1997, p. 613.
[9] W. Wiesenack, personal information.
[10] A.G. Croff, M.A. Bjerke, G.W. Morrison, L.M. Petrie, ORNL/TM-6051, 1978.
[11] U. Fischer, H.W. Wiese, KfK-3014, 1983.
[12] D.D. Lanning, C.E. Beyer, Modifications to NRC Fuel Rod Material Properties and Performance Models due to High Burnup, Pacific Northwest National Laboratories, 1997, in preparation.
[13] T. Kameyama, T. Matsumura, M. Kinoshita, Enlarged Halden Programme Group meeting on fuel performance experiments and analysis and computerised man–machine communication, Bolkesjö, Norway, HPR-336/3, 1990.
[14] OECD/NEA, JEF-2.2 Data Libraries, 1992.
[15] C.T. Walker, T. Kameyama, S. Kitajima, M. Kinoshita, J. Nucl. Mater. 188 (1992) 73.
[16] I. Misfeldt, The D-COM blind problem on fission gas release: experimental description and results, Summary report on OECD-NEA-CSNI/IAEA Specialists' Meeting on Water Reactor Fuel Safety and Fission Product Release in Off-Normal and Accident Conditions, IAEA-IWGFPT/16, 1983, p. 411.
[17] Water reactor fuel element computer modelling, Proceedings of a Specialists' Meeting, Bowness-on-Windermere, IAEA IWGFPT/19, 1984, p. 63.
[18] P. Knudsen, C. Bagger, H. Carlsen, I. Misfeldt, M. Mogensen, Final report on the Risø Fission Gas Project, Risø-FGP-R17rev, 1983.
[19] P. Knudsen, C. Bagger, H. Carlsen, B.S. Johansen, I. Misfeldt, M. Mogensen, Final report on the Risø Transient Fission Gas Project, Risø-TFGP-R29, Vol. 1, 1986.

[20] C.T. Walker, in: J.L. Lábár, E. Heikinheimo, P. Nicholson (Eds.), Proc. 2nd Regional, EMAS Workshop on Electron Probe Microanalysis of Materials Today—Practical Aspects, Kossuth Lajos University, Debrecen, Hungary, 1996, p. 102.
[21] I. Farthing, G. Love, V.D. Scott, C.T. Walker, Mikrochem. Acta Suppl. 12 (1992) 117.
[22] V.D. Scott, G. Love, X-Ray Spectrom. 21 (1992) 27.
[23] C.T. Walker, J. Nucl. Mater. 80 (1979) 190.
[24] C. Ronchi, C.T. Walker, J. Phys. D 13 (1980) 2175.
[25] C.T. Walker, C. Bagger, M. Mogensen, J. Nucl. Mater. 240 (1996) 32.